

# Poly(propylene)–Poly(propylene)-Grafted Maleic Anhydride–Organic Montmorillonite (PP–PP-g-MAH–Org-MMT) Nanocomposites. II. Nonisothermal Crystallization Kinetics

Weibing Xu,<sup>1,3</sup> Guodong Liang,<sup>1</sup> Wei Wang,<sup>1</sup> Shupeitang,<sup>1</sup> Pingsheng He,<sup>2</sup> Wei-Ping Pan<sup>3</sup>

<sup>1</sup>Department of Polymer Science and Engineering, Hefei University of Technology, Hefei, 230009 Anhui, China

<sup>2</sup>Department of Polymer Science and Engineering, University of Science and Technology of China, Hefei 230026, Anhui, China

<sup>3</sup>Material Characterization Center, Department of Chemistry, Western Kentucky University, Bowling Green, Kentucky 42101

Received 27 February 2002; revised 29 July 2002; accepted 29 July 2002

**ABSTRACT:** The nonisothermal crystallization kinetics of poly(propylene) (PP), PP–organic-montmorillonite (Org-MMT) composite, and PP–PP-grafted maleic anhydride (PP-g-MAH)–Org-MMT nanocomposites were investigated by differential scanning calorimetry (DSC) at various cooling rates. Avrami analysis modified by Jeziorny and a method developed by Mo well-described the nonisothermal crystallization process of these samples. The difference in the exponent  $n$  between PP and composite (either PP–Org-MMT or PP–PP-g-MAH–Org-MMT) indicated that nonisothermal kinetic crystallization corresponded to tridimensional growth with heterogeneous nucleation. The values of half-time,  $Z_c$ ; and  $F(T)$  showed that the crystallization rate increased with the increasing of cooling rates for PP and composites, but the crystallization rate of composites was

faster than that of PP at a given cooling rate. The method developed by Ozawa can also be applied to describe the nonisothermal crystallization process of PP, but did not describe that of composites. Moreover, the method proposed by Kissinger was used to evaluate the activation energy of the mentioned samples. The results showed that the activation energy of PP–Org-MMT was much greater than that of PP, but the activation energy of PP–PP-g-MAH–Org-MMT was close to that of pure PP. Overall, the results indicate that the addition of Org-MMT and PP-g-MAH may accelerate the overall nonisothermal crystallization process of PP. © 2003 Wiley Periodicals, Inc. *J Appl Polym Sci* 88: 3093–3099, 2003

**Key words:** poly(propylene) (PP); nanocomposites; crystallization; kinetics (polym.)

## INTRODUCTION

Studies of the crystallization process for polymers are generally limited to isothermal conditions because the theoretical analysis is easy to handle and problems associated with cooling rates and thermal gradients within specimens are avoided. The isothermal crystallization process of several polymers, such as polyoxymethylene (POM),<sup>1</sup> syndiotactic poly(propylenes),<sup>2</sup> poly(propylene) (PP) and maleic anhydride-grafted PP (PP-g-MAH),<sup>3</sup> have been studied. In practice, however, crystallization in a continuously changing thermal environment is of great interest because industrial processes generally proceed under nonisothermal conditions. Therefore, more and more attention has been paid to the study of the nonisothermal crystallization process for polymers.<sup>4–8</sup>

PP is a semicrystalline polymer. The final properties of composites based on PP in an engineering applica-

tion are critically dependent on the extent of crystallinity and the nature of crystalline morphology of PP, which in turn depend on the processing conditions. It is therefore necessary to understand the relationship between processing conditions and the development, nature, and degree of crystallinity of composites based on PP.

Since the Toyota group developed a montmorillonite–nylon nanocomposite with excellent mechanical properties, the use of a clay mineral as a reinforcement material for polymer nanocomposites has aroused great interest.<sup>9–11</sup> PP is one of the most widely used polyolefin polymers, so preparing nanocomposites based on PP has great economic potential for producing commodities. To date, many studies<sup>12–15</sup> about nanocomposition based on PP have been reported, but most concentrate on physical and mechanic properties. In our previous work, we successfully prepared PP–PP-g-MAH–Org-MMT via direct melt intercalation. In this paper several nonisothermal crystallization kinetic equations were used to study the crystallization characteristics of PP, PP–Org-MMT, and PP–PP-g-MAH–Org-MMT. Dynamic differential scanning

Correspondence to: W. B. Xu (xwb105105@sina.com).

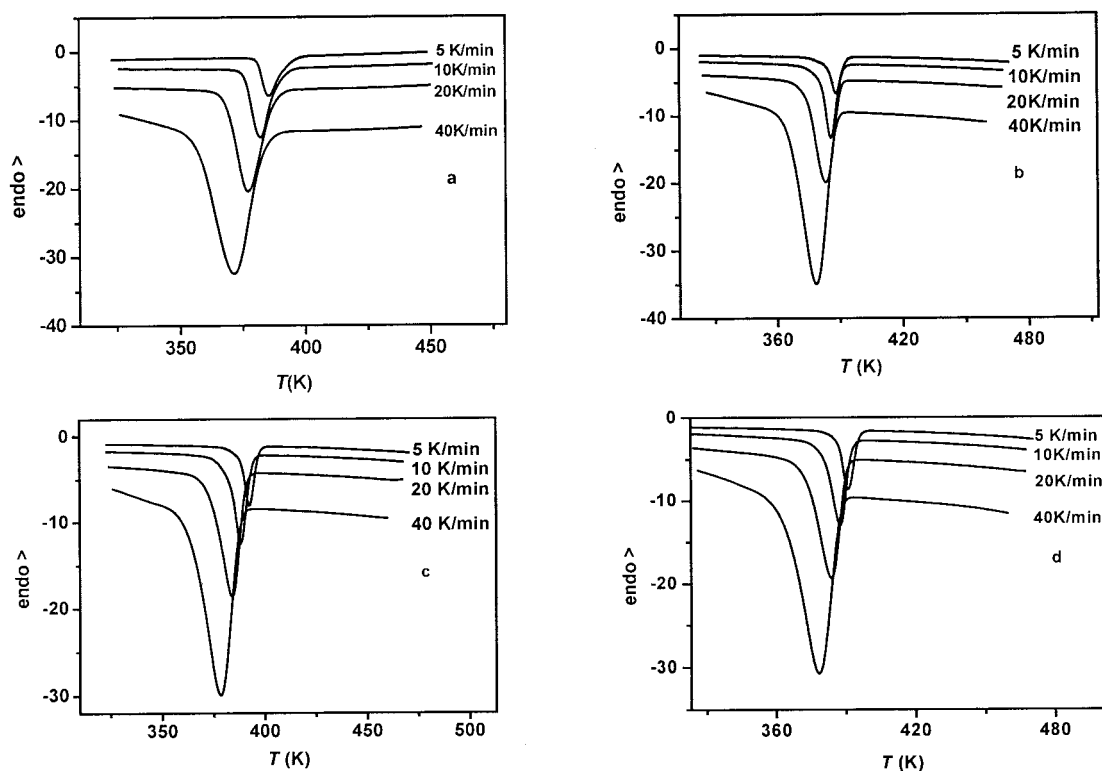


**Figure 1** DSC patterns for PP and PP-PP-g-MAH-Org-MMT during the nonisothermal crystallization process: (a) PP, (b) PP-Org-MMT (98 : 2), (c) PP-PP-g-MAH-Org-MMT (88 : 10 : 2), (d) PP-PP-g-MAH-Org-MMT (78 : 20 : 2).

calorimetry (DSC) thermograms supplied the necessary data. The activation energies of the crystallization of PP, PP-Org-MMT, and PP-PP-g-MAH-Org-MMT were also calculated by an evaluation proposed by Kissinger.<sup>16</sup>

## EXPERIMENTAL

### Nonisothermal DSC analysis

A Mettler Toledo DSC-821E apparatus was used for measuring nonisothermal crystallization kinetics in the cooling mode from the molten state (melt-crystallization). The temperature and energy readings were calibrated with indium at each cooling rate employed in the measurements. All measurements were carried out in a nitrogen atmosphere. The raw samples, pure PP, PP-Org-MMT (98 : 2), PP-PP-g-MAH-Org-MMT (88 : 10 : 2), PP-PP-g-MAH-Org-MMT (78 : 20 : 2), were prepared by the mold process described in our previous paper.<sup>17</sup> The nonisothermal melt crystallization was initiated by first heating the raw samples to 200°C for 5 min in the cell to eliminate previous thermal history. Then, the samples were cooled at constant rates of 5, 10, 20, or 40 K/min. The exothermic crystallization peak was then recorded as a function of temperature.

## RESULTS AND DISCUSSION

### Crystallization behavior of PP and PP-PP-g-MAH-Org-MMT nanocomposites

The crystallization exotherms of PP, PP-Org-MMT, and PP-PP-g-MAH-Org-MMT nanocomposites at various cooling rates are presented in Figure 1. Some useful parameters, such as the peak temperature ( $T_p$ ) and relative crystallinity ( $X_t$ ) as a function of crystallization temperature can be obtained from these curves to describe the nonisothermal crystallization behavior of PP, PP-Org-MMT, and PP-PP-g-MAH-Org-MMT. First, it is clearly seen from Figure 1 that  $T_p$  shifts, as expected, to lower temperature with increasing cooling rate for pure PP, PP-Org-MMT, and PP-PP-g-MAH-Org-MMT. This result can be explained as follows: the lower time scale causes the polymer to crystallize as the cooling rate is increased, which results in a need for a higher undercooling to initiate crystallization. In addition the motion of PP molecules cannot follow the cooling temperature when the specimens are cooled quickly. Second, for a given cooling rate,  $T_p$  of PP-Org-MMT composites is higher than that of pure PP as shown in Table I. This result can be explained by the heterogeneous nucleation effect of the Org-MMT particle on PP macromolecule segments. Melted PP macromolecule segments can be

TABLE I  
Nonisothermal Crystallization Kinetic Parameters

Sample	$\phi$ (K/min)	$n$	$Z_c$	$t_{1/2}$ (s)	$T_p$ (K)
PP	5	2.3	0.533	158.0	386.0
	10	2.5	0.836	84.4	382.0
	20	2.9	0.997	46.0	377.0
	40	3.1	1.041	29.9	371.5
PP-Org-MMT (98 : 2)	5	3.1	0.728	88.0	388.3
	10	3.0	1.048	44.7	385.8
	20	2.9	1.106	26.1	383.2
	40	3.5	1.107	17.3	378.3
PP-PP-g-MAH-Org-MMT (88 : 10 : 2)	5	3.4	0.687	91.7	392.9
	10	3.0	1.011	51.1	388.2
	20	3.2	1.091	31.5	384.1
	40	3.5	1.099	19.8	378.1
PP-PP-g-MAH-Org-MMT (78 : 20 : 2)	5	3.1	0.711	87.6	391.1
	10	2.9	1.037	45.8	387.7
	20	3.1	1.188	27.5	383.7
	40	2.9	1.121	17.1	378.2

easily attached to the surface of the Org-MMT particle, which leads to the crystallization of PP molecules at a higher crystallization temperature. Moreover, the difference of  $T_p$  between PP-Org-MMT and PP-PP-g-MAH-Org-MMT indicates heterogeneous nucleus effects of PP-g-MAH and a synergetic effect between PP-g-MAH and Org-MMT on the crystallization behavior of PP. However, increasing the content of PP-g-MAH above 10 wt %, the concentration at which the highest  $T_p$  was obtained, results in a decrease in  $T_p$ .

#### Nonisothermal crystallization kinetics of PP and PP/PP-g-MAH/org-MMT

The relative degree of crystallinity,  $X_t$ , as a function of crystallization temperature  $T$  is defined as

$$X_t = \int_{T_0}^T (dH_c/dT)dT / \int_{T_0}^{T_\infty} (dH_c/dT)dT \quad (1)$$

where  $T_0$  and  $T_\infty$  represent the onset and end of crystallization temperatures, respectively, and  $H_c$  is the enthalpy of crystallization.

The development of relative degree of crystallinity as a function of temperature for nanocomposite (PP/PP-g-MAH/Org-MMT = 88 : 10 : 2) at various cooling rates is shown in Figure 2. The plots of  $X_t$  versus  $T$  for PP and PP-Org-MMT are similar to that of the (PP-PP-g-MAH-Org-MMT 88 : 10 : 2) nanocomposite. All these curves have the same sigmoidal shape, implying that only the lag effect of cooling rate on crystallization is observed. The horizontal temperature axis in Figure 2 can be transferred into a time scale (Fig. 3) by the equation  $t = (T_0 - T)/\phi$  (where  $T$  is the temperature at crystallization time  $t$ , and  $\phi$  is the cooling rate). Expressed as such, the results show that the higher the cooling rate, the shorter the time for com-

pleting crystallization. The half-times of nonisothermal crystallization ( $t_{1/2}$ ) obtained from Figure 3 for PP, PP-Org-MMT, and PP-PP-g-MAH-Org-MMT are listed in Table I. As expected, the value of  $t_{1/2}$  decreases with increasing cooling rates for PP, PP-Org-MMT, and PP-PP-g-MAH-Org-MMT. Moreover, at a given cooling rate, the value of  $t_{1/2}$  for PP-Org-MMT is lower than that for PP, signifying that the addition of Org-MMT accelerated the overall crystallization process. However, the  $t_{1/2}$  value of PP-PP-g-MAH-Org-MMT is close to that of PP-Org-MMT because the heterogeneous nucleation effect of the carboxyl in PP-g-MAH and the spacial obstacle effect caused by the branched chain in PP-g-MAH offset each other. Therefore, the value of  $t_{1/2}$  does not benefit from the addition of PP-g-MAH.

Assuming that nonisothermal crystallization process may be composed of infinitesimally small isother-

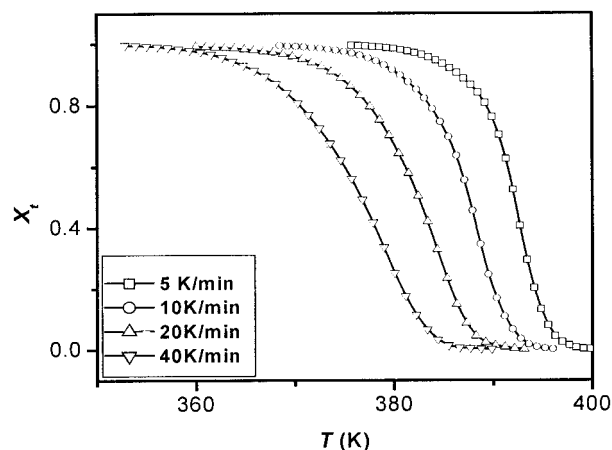
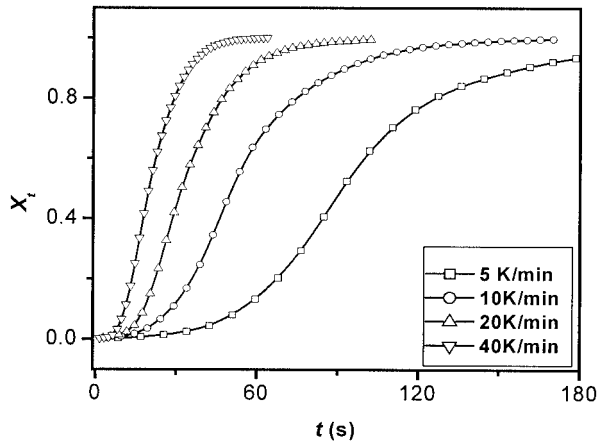


Figure 2 Patterns of  $X_t$  versus  $T$  during the nonisothermal crystallization process of PP-PP-g-MAH-Org-MMT (88 : 10 : 2).



**Figure 3** Plots of  $X_t$  versus  $t$  during the nonisothermal crystallization process of PP-PP-g-MAH-Org-MMT (88 : 10 : 2).

mal crystallization steps, Ozawa<sup>8</sup> extended the Avrami equation to the nonisothermal case as follows:

$$1 - X_t = \exp(-K(T)/\phi^m) \quad (2)$$

where  $K(T)$  is the function of cooling rate,  $\phi$  is the cooling rate, and  $m$  is the Ozawa exponent, which depends on the dimension of the crystal growth. The double-logarithmic form of eq 2 is

$$\ln[-\ln(1 - X_t)] = \ln K(T) - m \ln \phi \quad (3)$$

A plot of  $\ln[-\ln(1 - X_t)]$  against  $\ln \phi$  at a given temperature should result in a straight line if the Ozawa method is valid. Thus,  $K(T)$  and  $m$  can be estimated from the intercept and slope, respectively. The results based on Ozawa method are shown in Figure 4 and Table II. The curves in the plots of  $\ln[-\ln(1 - X_t)]$  versus  $\ln \phi$  for PP exhibit a better

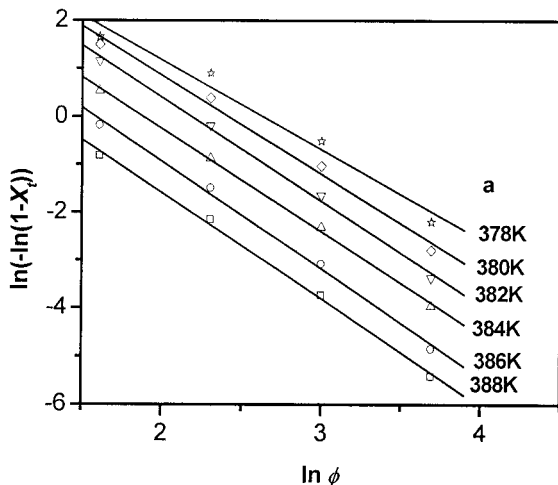


**TABLE II**  
Nonisothermal Crystallization Kinetic Parameters for PP at Different Temperatures

Temperature (K)	$m$	$K(T)$
388	2.22	17.28
386	2.25	35.16
384	2.15	57.97
382	2.17	114.43
380	2.06	145.47
378	1.87	135.64

linear relationship, but those of the composites PP-Org-MMT and PP-PP-g-MAH-Org-MMT do not. These results show that PP can be analyzed by the Ozawa method but that PP-PP-g-MAH-Org-MMT can not. The reason for this difference is that at a given temperature, the crystallization processes for PP-PP-g-MAH-Org-MMT are at different stages at different cooling rates; that is, the lower cooling rate process is towards the end of the crystallization process, whereas the higher cooling rate process is at an early stage of the crystallization process. The addition of Org-MMT and PP-g-MAH magnify the influence of cooling rate on the crystallization process.

The alternative approach adopted here was Avrami equation:<sup>18</sup>

$$1 - X_t = \exp(-Z_t t^n) \quad (4)$$

where the exponent  $n$  is a mechanism constant that depends on the type of nucleation and growth process parameters, and  $Z_t$  is a composite rate constant involving both nucleation and growth rate parameters. Using eq. 4 in the double-logarithmic form,

$$\ln[-\ln(1 - X_t)] = \ln Z_t + n \ln t \quad (5)$$

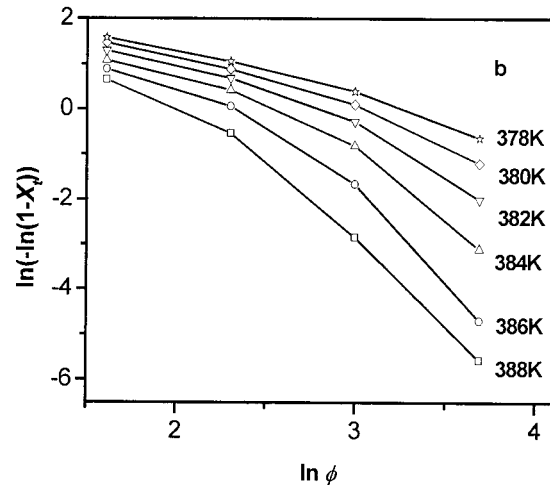


**Figure 4** Plots of  $\ln[-\ln(1 - X_t)]$  versus  $\ln \phi$  during the nonisothermal crystallization process: (a) PP; (b) PP-PP-g-MAH-Org-MMT (88 : 10 : 2).

and plotting  $\ln[-\ln(1 - X_t)]$  against  $\ln t$  for each cooling rate, a straight line is obtained with the data at a low degree of crystallinity in the linear regression only (see Fig. 5). Thus, two adjustable parameters,  $Z_t$  and  $n$ , can be estimated. It should be taken into account that in nonisothermal crystallization,  $Z_t$  and  $n$  do not have the same physical significance as in the isothermal crystallization because under nonisothermal crystallization, the temperature changes constantly. This constant change affects the rates of both nuclei formation and spherulite growth, both of which are temperature dependent. In this case,  $Z_t$  and  $n$  are two adjustable parameters only to be fit to the data. Although the physical meanings of  $Z_t$  and  $n$  cannot be related in a simple way to the nonisothermal case, eq. 4 can still provides further insight into the kinetics of nonisothermal crystallization.

Considering the nonisothermal character of the process investigated, the final form of the parameter characterizing the kinetics of nonisothermal crystallization was given by Jeziorny:<sup>7</sup>

$$\ln Z_c = \ln Z_t / \phi \quad (6)$$

The results obtained from the Avrami plots and the Jeziorny method are listed in Table I. The exponent  $n$  of varied from 2.3 to 3.1 for PP and from 2.9 to 3.5 for PP-Org-MMT and PP-PP-g-MAH-Org-MMT. Although the exponent  $n$  in nonisothermal crystallization displayed a wide range of values and was more scattered than those obtained from isothermal crystallization,<sup>19</sup> it is interesting that the exponent  $n$  for PP-Org-MMT was larger than that for PP at every cooling rate. This result shows that the Org-MMT acted as a nucleating agent in the PP matrix. In contrast, the exponent  $n$  of PP-PP-g-MAH-Org-MMT is similar to that of PP-Org-MMT, indicating that the nonisother-

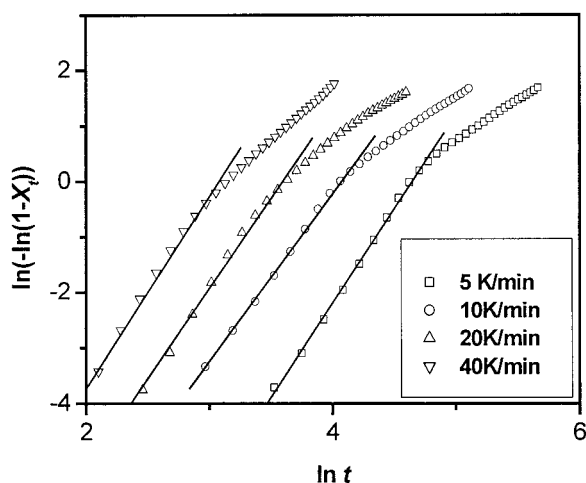


**Figure 5** Plots of  $\ln[-\ln(1 - X_t)]$  versus  $\ln t$  during the nonisothermal crystallization process for PP-PP-g-MAH-Org-MMT (88 : 10 : 2).

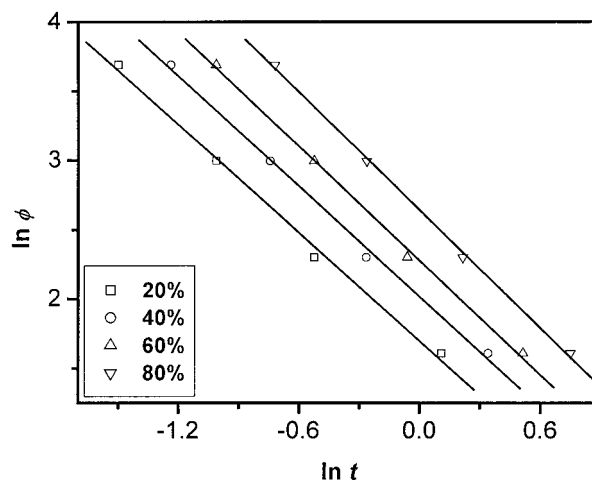


**Figure 6** Plots of  $\ln \phi$  versus  $\ln t$  during the nonisothermal crystallization process for PP-PP-g-MAH-Org-MMT (88 : 10 : 2).

mal crystallization of PP-PP-g-MAH-Org-MMT corresponds to tridimensional growth with heterogeneous nucleation, like that of PP-Org-MMT. For both PP and composites (either PP-Org-MMT or PP-PP-g-MAH-Org-MMT), as expected, the value of  $Z_c$  increases with increasing cooling rates.

A method developed by Mol and co-workers<sup>20</sup> was employed to describe the nonisothermal crystallization to make a comparison. The physical variables relating to the nonisothermal crystallization process are relative degree of crystallinity ( $X$ ), cooling rate ( $\phi$ ), and crystallization temperature ( $T$ ). Both Ozawa and Avrami equations give the relationship:

$$\ln Z_t + n \ln t = \ln K(T) - m \ln \phi \quad (7)$$

At a given crystallinity  $X_t$ , eq. 7 can be rearranged to

$$\ln \phi = \ln F(T) - a \ln t \quad (8)$$

where  $F(T) = [K(T)/Z_t]^{1/m}$  refers to the value of cooling rate, which must be chosen within a unit of crystallization time when the measured system amounts to a certain degree of crystallinity; and  $a$  is the ratio of the Avrami exponent  $n$  to Ozawa exponent  $m$  ( $n/m$ ). According to eq. 8, at a given degree of crystallinity, plotting  $\ln \phi$  versus  $\ln t$  (Fig. 6) yields a linear relationship between  $\ln \phi$  and  $\ln t$ . The kinetic parameter  $F(T)$  and  $a$  are determined from the intercept and slope of the lines. The results of such an analysis are listed in Table III for PP and PP-PP-g-MAH-Org-MMT. The value of  $a$  varies from 1.22 to 1.32 for PP, from 1.21 to 1.33 for PP-Org-MMT, and from 1.30 to 1.42 for PP-PP-g-MAH-Org-MMT. The value of  $F(T)$  systematically increases with increasing relative degree of crystallinity. At the same relative degree of crystallinity, the  $F(T)$  for PP-Org-MMT is smaller than that for PP,

which indicates that PP-Org-MMT crystallizes at a quicker rate than PP. Moreover, the value of  $F(T)$  for PP-PP-g-MAH-Org-MMT is close to that of PP-Org-MMT, which indicates that the PP-g-MAH in PP-PP-g-MAH-Org-MMT does not contribute to a quicker crystallization rate. This conclusion agrees with the one drawn from Avrami analysis. Obviously, this approach is successful in describing the nonisothermal crystallization process of PP and composites (both PP-Org-MMT and PP-PP-g-MAH-Org-MMT), as shown for poly(ether ether ketone) (PEEK),<sup>20</sup> poly(hydroxybutyrate)-poly(vinyl acetate) (PHB-PVAc) blends,<sup>21</sup> and POM-Org-MMT nanocomposites.<sup>22</sup>

Another method often used for evaluation of activation energy at various cooling rates, based on eq. 9, was proposed by Kissinger:<sup>16</sup>

$$\frac{d[\ln(\phi/T_p^2)]}{d(1/T_p)} = -\frac{\Delta E}{R} \quad (9)$$

where  $R$  is the universal gas constant and  $\Delta E$  is the activation energy of crystallization. The activation energies of the nonisothermal melt crystallization of PP and composites (listed in Table III), were calculated with the data from a plot of  $\ln(\phi/T_p^2)$  versus  $1/T_p$  (Figure 7). The value of  $\Delta E$  for PP-Org-MMT is much larger than that for PP because the Org-MMT particle increases the viscosity of PP, which prevents the PP macromolecule segment from rearranging, and as a result, increases the activation energy. However, the value of  $\Delta E$  for PP-PP-g-MAH-Org-MMT is smaller than that of PP-Org-MMT the macromolecule segments in PP-PP-g-MAH-Org-MMT intercalated into layers of Org-MMT, which are highly restrained and

**TABLE III**  
Nonisothermal Crystallization Kinetic Parameters at Different Relative Degree of Crystallinity

Sample	$X_t$ (%)	$a$	$F(T)$	$\Delta E$ (kJ/mol)
PP	20	1.25	11.02	175.7
	40	1.22	14.44	
	60	1.25	17.29	
	80	1.32	21.11	
PP-Org-MMT (98 : 2)	20	1.21	5.00	257.5
	40	1.25	6.69	
	60	1.33	8.58	
	80	1.28	11.70	
PP-PP-g-MAH-Org-MMT (88 : 10 : 2)	20	1.30	5.47	181.6
	40	1.32	7.54	
	60	1.37	9.78	
	80	1.42	14.01	
PP-PP-g-MAH-Org-MMT (78 : 20 : 2)	20	1.20	5.05	203.2
	40	1.23	6.82	
	60	1.31	8.76	
	80	1.41	12.18	

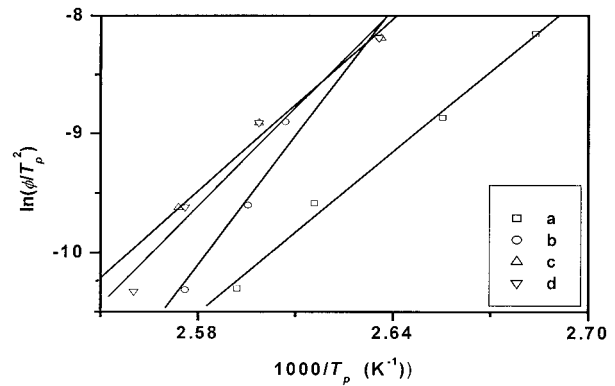


**Figure 7** Plotting of  $\ln(\phi/T_p^2)$  versus  $1/T_p$  during the nonisothermal crystallization process: (a) PP; (b) PP-Org-MMT (98 : 2); (c) PP-PP-g-MAH-Org-MMT (88 : 10 : 2); (d) PP-PP-g-MAH-Org-MMT (78 : 20 : 2).

which easily form nucleation seeds. In addition the carboxyl group can act as a nucleation agent during the crystallization process. These facts result in a decrease in the activation energy of PP-PP-g-MAH-Org-MMT which was close to that of pure PP. A further increase in the content of PP-g-MAH resulted in a slight increase in the activation energy of PP-PP-g-MAH-Org-MMT.

## CONCLUSION

The PP-PP-g-MAH-Org-MMT nanocomposite was successfully prepared by melt intercalation. Ozawa analysis provides an adequate description of the nonisothermal crystallization of PP but not that of PP-PP-g-MAH-Org-MMT. Avrami analysis as modified by Jeziorny and a method developed by Mo were successful in describing the nonisothermal crystallization process of PP and both composites (PP-Org-MMT and PP-PP-g-MAH-Org-MMT). The difference between the exponent  $n$  for PP and those for either composite (PP-Org-MMT or PP-PP-g-MAH-Org-MMT) indicates that nonisothermal kinetic crystallization consists of tridimensional growth with heterogeneous nucleation. The half-time  $t_{1/2}$ ,  $Z_c$ , and  $F(T)$  parameters showed that the crystallization rate of PP and composites increased with increasing cooling rates, that the crystallization rate of composites was faster than that of PP at a given cooling rate, and that the difference in the crystallization rate between PP-PP-g-MAH-Org-MMT and PP-Org-MMT was not significant. The activation energy of PP-Org-MMT was much greater than that of PP, but the activation energy of PP-PP-g-MAH-Org-MMT is close to that of pure PP. Overall, the results show that the addition of Org-MMT and PP-g-MAH may accelerate the nonisothermal crystallization process of PP.

The authors gratefully acknowledge the financial support (Grant Number: 01402012) of the Committee of Science and Technology of Anhui Province, China.

## References

1. Xu, W. B.; He, P. S. *J Appl Polym Sci* 2001, 80, 304.
2. Supaphol, P.; Spruiell, J. E. *Polymer* 2000, 41, 1205.
3. Seo, Y.; Kim, J.; Kim, K. U.; Kim, Y. C. *Polymer* 2000, 41, 2639.
4. Xu, W. B.; Ge, M. L.; He, P. S. *J Polym Sci, Part B: Polym Phys* 2002, 40, 408.
5. Markus, L. *Polym Eng Sci* 1998, 38, 610.
6. Nakamura, K.; Watanabe, T.; Katayama, K.; Amano, T. *J Appl Polym Sci* 1972, 16, 1077.
7. Jeziorny, A. *Polymer* 1978, 19, 1142.
8. Ozawa, T. *Polymer* 1971, 12, 150.
9. Wang, K. H.; Choi, M. H.; Koo, C. M.; Choi, Y. S.; Chung, I. J. *Polymer* 2001, 42, 9819.
10. Fukushima, Y.; Okada, A.; Kawasumi, M.; Kurauchi, T.; Kamigaito, O. *Clay Miner* 1988, 23, 27.
11. Giannelis, E. P. *Adv Mater* 1996, 8, 29.
12. Kawasumi, M.; Hadegawa, N. *Macromolecules* 1997, 30, 6333.
13. Hambir, S.; Bulakh, N. *J Polym Sci, Part B: Polym Phys* 2001, 39, 446.
14. Gilman, J. W.; Jackson, C. L. *Chem Mater* 2000, 12, 1866.
15. Kato, K.; Usuki, A. *J Appl Polym Sci* 1997, 66, 1781.
16. Kissinger, H. E. *J Res Natl Bur Stand (US)* 1956, 57, 217.
17. Xu, W.; Liang, G.; Wang, W.; Tang, S.; He, P.; Pan, W.-P. *J Appl Polym Sci*, to appear.
18. Avrami, M. J. *Chem Phys* 1941, 9, 177.
19. Srinivas, S.; Babu, J. R.; Riffle, J. S.; Wilkes, G. L. *Polym Eng Sci* 1997, 37, 497.
20. Liu, T. X.; Mo, Z. S.; Wang, S. E.; Zhang, H. F. *Polym Eng Sci* 1997, 37, 568.
21. An, Y.; Li, L.; Mo, Z. S.; Feng, Z. L. *J Polym Sci, Part B: Polym Phys* 1999, 37, 443.
22. Xu, W. B.; Ge, M. L.; He, P. S. *J Appl Polym Sci* 2001, 82, 2281.